RSC Advances

PAPER

View Article Online
View Journal | View Issue

Cite this: *RSC Adv.*, 2021, **11**, 33202

Fluorescent PEI@Pd nanoclusters: facile synthesis and application†

Wen Wen,[a] Zhongping Li,[a] Xu Wang,[b] Xiaoyan Du,[a] Guangming Wen*[ac] and Li Li*[d]

Received 20th August 2021
Accepted 26th September 2021

DOI: 10.1039/d1ra06307c

rsc.li/rsc-advances

Metal nanoclusters (NCs) have recently emerged as a novel class of luminescent nanomaterials and held significant potential in analytical chemistry. In this work, novel polyethyleneimine stabilized palladium nanoclusters (PEI–Pd NCs) were synthesized by chemical reduction at 60 °C for 6 h, and used as a fluorescent nanosensor for the detection of oxytetracycline (OTC). The spectral characteristics, surface structure and morphology of the Pd NCs were studied. The selectivity and stability of the nanosensor were also investigated. The experimental results showed that the Pd NCs had good biocompatibility, stability and photobleaching resistance in aqueous solution. The fluorescence quenching effect showed a good linear relationship with the degree of fluorescence quenching of Pd NCs and OTC in the range of 25–440 nM, with a correlation coefficient of 0.99. The limit of detection (LOD) of the proposed nanosensor for OTC was calculated to be 22 nM. The mechanism of determination was thought to be an inner filter effect (IFE) between OTC and Pd NCs. Based on this, we have established a new nanosensing analysis method for detecting OTC.

1. Introduction

Owing to their potent antibacterial properties, low cost and low side effects, antibiotics have been widely applied in the prevention and treatment of diseases as well as in agriculture fields.[1,2] However, the abuse of antibiotics not only leads to the residue of antibiotics in animal-origin foodstuffs, but also aggravates environmental pollution.[3] Eventually, they can cause a variety of health problems in humans, such as genetic defects, cancer, immunity decline, and allergic reactions.[4,5]

As a broad spectrum antibiotic, oxytetracycline (OTC) has become one of the most commonly used tetracycline antibiotics for the treatment of livestock infections.[6] However, there are many reports and confirmed cases of OTC residues due to overuse of this common antibiotic. Monitoring results of veterinary medicinal product residues and other substances in live animals and animal products in 2015 indicated that OTC was one of the most frequent antimicrobials tested for substandard samples.[7] Since OTC cannot be completely absorbed and utilized by an organism, it is excreted along with metabolites, which inevitably leads to the destruction of the ecological environment.[8] Wang *et al.* first investigated the distribution of 13 common antibiotics in the waters of Lake Honghu, and the results showed that the concentration of OTC in the samples ranked among the top three.[9] The most critical adverse effect of antibiotic residues is antibiotic resistance, which is transferred to the human body due to the mobility of resistance.[10] The AMR (antimicrobial resistance) Industry Alliance defined safe levels for various antibiotics as between 20 and 32 000 ng L^{-1}, depending on the specific substance. Therefore, there is a need to develop highly sensitive and selective methods to monitor OTC in the environment and to identify residues in foods.

Until now, various analytical techniques including high-performance liquid chromatography (HPLC),[11] liquid chromatography-mass spectrometry (LC-MS),[12] electro-chemistry,[13,14] electro-chemiluminescence (ECL),[15] colorimetric analysis,[16,17] enzyme linked immunosorbent assay (ELISA),[18] microbiological and chemical detection,[19] and fluorescence method,[20,21] have been devised to determine OTC. Although the detection method based on chromatography can obtain high accuracy and stability results, the instruments used are expensive and complicated to operate, which is not suitable for universal application in practical work. ELISA and microbiological methods are suitable for sample screening because of their fast detection speed and low detection limit, but they may have problems in accurate quantitation due to the interference of complex sample matrices.[22,23] In addition, electro-chemistry and ECL are widely used in the detection of antibiotics in food and environmental filed. However, the service life and long-term stability of relevant sensors need be improved.[24] With the improvement of nanotechnology, metal nanosensors have shown certain advantages in antibiotic detection.

[a]*Institute of Environmental Science, School of Chemistry and Chemical Engineering, Shanxi University, Taiyuan 030006, China. E-mail: zl104@sxu.edu.cn*

[b]*Shanxi Research Center for Information and Strategy of Science and Technology, Taiyuan 030024, China*

[c]*School of Chemistry and Chemical Engineering, Jinzhong University, Jinzhong, 030619, China*

[d]*First Hospital of Shanxi Medical University, Taiyuan 030001, China*

† Electronic supplementary information (ESI) available. See DOI: 10.1039/d1ra06307c

Metal nanoclusters usually consist of several to hundreds of metal atoms with particles close to the size of Fermi wavelength.[25] In recent years, metal nanoclusters have raised extensive research interest because of their unique function in bridging the "gap" between metal atoms and nanoparticles.[26] The most significant difference between metal nanoclusters and large-sized nanoparticles is that metal nanoclusters usually do not exhibit characteristic surface plasmon resonance absorption in the visible light region, but show fluorescence in the visible light to near-infrared region.[27] At the same time, metal nanoclusters have become a research hotspot because of their good optical stability, long fluorescence lifetime and high quantum yield.[28] Currently, nanoclusters, including gold nanoclusters (Au NCs), silver nanoclusters (Ag NCs), copper nanoclusters (Cu NCs), platinum nanoclusters (Pt NCs), molybdenum nanoclusters (Mo NCs), *etc.*, have been widely used in biology markers, single-molecule spectroscopy, catalysis, optical sensing, and other fields.[29] Although metal nanoclusters have been extensively studied in the past few years, there are few reports on fluorescent palladium nanoclusters (Pd NCs).[30] In previous research, our research group reported that polyvinylpyrrolidone (PVP) coated palladium nanoclusters (PVP–Pd NCs) Pd NCs were prepared and used as novel fluorescence nanosensors for detecting OTC.[31]

Herein, polyethyleneimine (PEI)-coated Pd NCs (PEI–Pd NCs) are used as nanosensors to detect OTC. In contrast to other well-known and stable gold–silver–copper nanoclusters detected by various templates, the selective and sensitive quench effect of OTC on the fluorescence of Pd NCs is reported for the first time. Based on the fluorescence resonance energy transfer interaction occurring between OTC and Pd NCs, the fluorescence signal of Pd NCs can be used as a signal indicator for the detection of OTC. The nanosensor boasts good selectivity and stability, and the sensing system has been successfully applied to detect OTC in real water samples. Moreover, PEI has been proven to be a substance with good biology compatibility and efficient gene delivery carrier both *in vitro* and *in vivo*. Therefore, this nanotechnology biology-compatible OTC probe would be a candidate for an effective and versatile sensor in the environmental, medicine and biotechnology fields.

2. Experimental

2.1. Reagents and material

Amoxicillin (AMX), kanamycin sulfate (KM), chloramphenicol (CHL), erythromycin (EM), oxytetracycline (OTC), ciprofloxacin (CIP) were purchased from Beijing Chemical Corp. (Beijing, China). Tetracycline (TC), ascorbic acid ($C_6H_8O_6$), polyethyleneimine (PEI), palladium nitrate ($Pd(NO_3)_2$) and anhydrous ethanol were purchased from Shanghai Aladdin Reagent Co., Ltd (Shanghai, China). All reagents were analytically pure without further purification.

2.2. Apparatus and instruments

The morphology and phase of the Pd NCs were characterized by a high-resolution transmission electron microscope with an acceleration voltage of 200 kV (HRTEM, JEM-2100, Japan). All TEM samples were prepared by depositing a drop of diluted suspension in ethanol on a copper grid coated with carbon film. An X-ray photoelectron spectrometer (XPS, AXIS ULTRA DLD, United Kingdom) was applied to characterize the chemical composition of the Pd NCs. The surface functional groups of Pd NCs were characterized with Fourier transform infrared (FTIR) spectroscopy. UV absorption spectra were recorded on a Shimadzu UV-265 spectrophotometer (Tokyo, Japan). Fluorescence spectra were written down on a Hitachi F4500 spectrofluorometer (Tokyo, Japan). Both excitation and emission slits were set at 10.0 nm.

2.3. Synthesis of Pd NCs

Put 0.2 mL of $Pd(NO_3)_2$ (100 mM) solution into 4.2 mL of PEI (25 mg mL^{-1}) solution, stirred it at constant speed for 10 min, then added 100 μL of ascorbic acid (1.5 M), and waited for the reaction at 60 °C for 6 h. The above solution was filtered through a 0.22 μm microporous filter membrane, and then centrifuged at a speed of 8000 rpm min^{-1} for 15 min. Then dialyzed the solution in a 1000 Da dialysis bag for 24 h to remove impurities. The resulting solution was stored at 4 °C and set aside. A schematic diagram of the synthesis is shown in Fig. 1.

2.4. Detection of OTC

Dilute 100 μL of Pd NCs solution in 1 mL of PBS buffer solution, then add 0.01 mL of OTC (0.01 M) and mix it sufficiently. In the same way, dilute 100 μL of Pd NCs solution in 1 mL of PBS buffer solution, then add 0.01 mL of AMX (0.1 M), KM (0.1 M), CIP (0.1 M), TC (0.1 M), CHL (0.1 M), and EM (0.1 M) solution of known concentrations, mix it sufficiently. Finally, measure the fluorescence intensity at 360 excitation wavelength and 495 nm emission wavelength.

3. Results and discussion

3.1. Optimization of experimental conditions

Reaction time and temperature often play a key role during Pd NCs synthesis. In this work, the effects of reaction time and reaction temperature on the properties of Pd NCs were investigated as shown in Fig. 2A and B, respectively. The fluorescence intensity of Pd NCs was increased and then decreased when the reaction time was set from 2 h to 10 h. In addition, when reaction time reached 6 h, the fluorescence intensity was the highest. The effect of temperature on the fluorescence properties of Pd NCs was studied by changing the reaction temperature from 40 °C to 80 °C under the same experimental conditions. The results

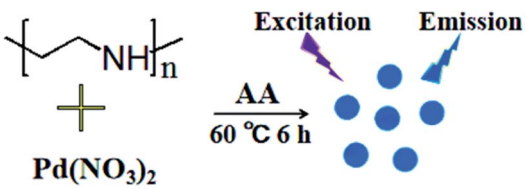

Fig. 1 Schematic diagram of the synthesis process of Pd NCs.

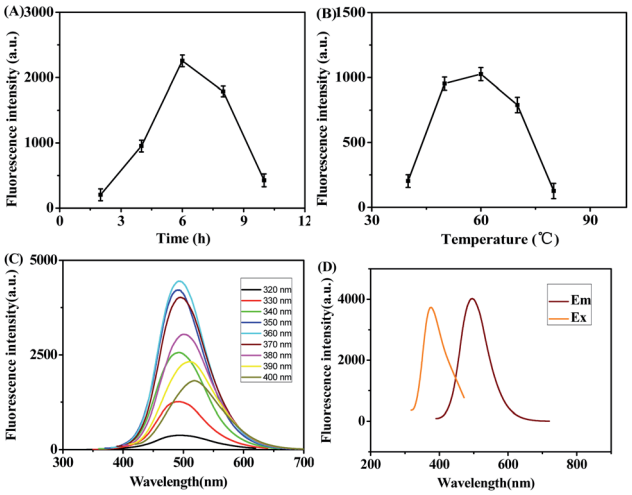

Fig. 2 Different reaction time (A) and reaction temperature (B) of Pd NCs. (C) Fluorescence spectra of Pd NCs at different excitation wavelengths. (D) Excitation and emission spectra of Pd NCs.

showed that the fluorescence intensity of Pd NCs also showed a general trend of increasing and then decreasing with the change of reaction temperature from 40 °C to 80 °C, and the fluorescence intensity was highest at 60 °C. So the reaction condition of 6 h at 60 °C was used to synthesize fluorescent Pd NCs in this experiment. The property of fluorescence spectra of Pd NCs were investigated in Fig. 2C and D. As the fluorescence spectra shown in Fig. 2C, the excitation wavelength of Pd NCs was set between 320 nm and 400 nm, and the fluorescence intensity of Pd NCs increased at first and then decreased, showing a weak excitation wavelength dependence, which was probably due to the relatively uniform size of the prepared Pd NCs. The optimal excitation wavelength was 360 nm and the optimal emission wavelength was 495 nm (Fig. 2D).

3.2. Characterization and properties of Pd NCs

The morphology of Pd NCs was imaged under transmission electron microscope (TEM). It was observed that the prepared Pd NCs were nearly spherical with good dispersion and homogeneous morphology with an average particle size of 1.35 nm (Fig. 3A). Among them, only small diameter particles and few particles edge have broken, which may be caused by the shock of cryopreservation during the preparation of samples for TEM observation. Naik, *et al.* (2017) also reported the similar observation.[32] As seen in the image on the right side of the Fig. 3A (inset), the collected particle size distribution data was presented in the form of histogram to analyze the particle size distribution. Pd NCs with a particle size of 1.35 nm dominated, confirming the uniformity of Pd NCs particle size. However, the obvious aggregation was observed after reaction with OTC (Fig. S1†). The surface functional groups of Pd NCs were characterized by FTIR spectroscopy (Fig. 3B). Pure Pd NCs had four features at 3400 cm^{-1}, 1668 cm^{-1}, 1489 cm^{-1}, and 1435 cm^{-1}; the absorption band at 3400 cm^{-1} was attributed to the stretching vibration of N–H; the bands at 1668 cm^{-1} and

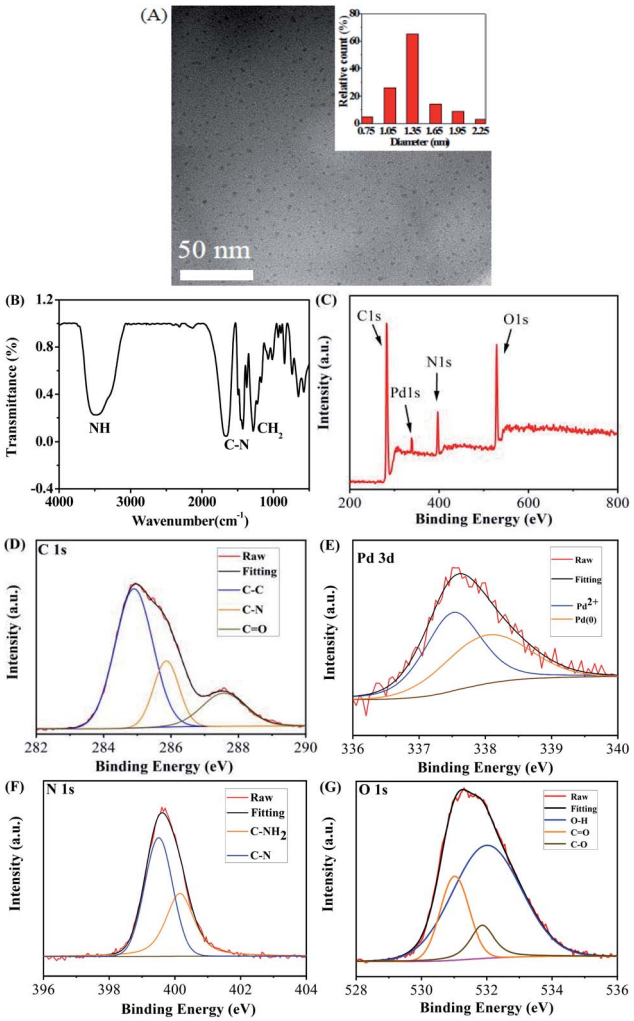

Fig. 3 (A) The TEM image of Pd NCs (inset: particle size distribution). (B) FTIR spectra of Pd NCs. (C) Overall XPS spectra of Pd NCs and individual XPS C 1s (D), Pd 3d (E), N 1s (F) and O 1s (G).

1489 cm^{-1} were caused by the bending vibration of C–N; and the bending vibration peak of CH_2 was at 1435 cm^{-1}.[33–37] The XPS spectra further illustrated the composition of Pd NCs as shown in Fig. 3C. Pd NCs contained four main peaks at 284.8 eV, 337.4 eV, 398.9 eV, and 531.2 eV, corresponding to C 1s, Pd 3d, N 1s and O 1s (Fig. 3D–G). C 1s peaks appeared at 284.9 eV, 285.8 eV and 286.3 eV, which were attributed to C–C, C–N and C–O bonds, respectively (Fig. 3D). As shown in Fig. 3E, Pd 3d was composed of two valence states. Among them, Pd^{1+} was a strong peak at 337.53 eV, because Pd^{1+} was distributed on the outer surface of Pd cluster nucleus after forming Pd–N bond with the amino group on PEI. The other was reduced Pd^{0} at 338.07 eV, probably mainly concentrated in the core of the metal cluster. The spectra of N 1s were decomposed into two peaks indicating the existence of two different types of nitrogen (Fig. 3F). The peaks at 399.5 eV and 400.1 eV can represent C–N and C–NH_2, respectively. O 1s spectra showed three peaks at 531.0 eV, 531.8 eV and 532.0 eV, corresponding to C=O, C–O and O–H, respectively (Fig. 3G).

3.3. Stability of Pd NCs

The stability of Pd NCs was investigated in terms of pH, ion concentration, resistance to photonic bleaching and storage time. As shown in Fig. 4A, the fluorescence intensity of Pd NCs gradually enhanced with the increase of pH, and reached the highest when the pH was in the range of 6.0–10.0; when the pH was greater than 11.0, the fluorescence intensity decreased, indicating that this Pd NCs was suitable for biological systems, and the buffer system with pH = 7.0 was chosen in this work. The fluorescence intensity of Pd NCs showed no significant difference in NaCl solution with different concentrations (Fig. 4B), which not only indicated that the Pd NCs were insensitive to the change of salt concentration and were salt-resistant, but also indicated that the Pd NCs had stability in 0–5 mol L^{-1} NaCl solution. Then, the fluorescence stability of our Pd NCs was expored under continuous illumination for 150 min. According to Fig. 4C, the fluorescence intensity remained basically unchanged within 0–150 min of illumination, demonstrating that Pd NCs had good photostability. In addition, the Pd NCs retained above 92.90% of its original fluorescence intensity after 6 months of storage in a 4 °C refrigerator, indicating that the Pd NCs had good storage stability (Fig. 4D).

3.4. Sensitive detection of OTC by Pd NCs

The key factors for evaluating nanosensors are sensitivity and selectivity. The prepared fluorescence sensor was used to measure the fluorescence intensity by studying the effects of different antibiotics on the fluorescence intensity of Pd NCs. Different antibiotics, including AMX, KM, CIP, TC, CHL, and EM with 10 times OTC concentration were dissolved in 1 mL of PBS to determine the specificity of the nanosensor. The results were shown in Fig. 5A. Except for OTC, other antibiotics of ultra-high concentrations still not interfere with the fluorescence intensity of Pd NCs, indicating high sensitivity and selectivity of the sensor. And the UV spectrum (AMX, KM, CIP, TC, CHL, EM and OTC) and selectivity of fluorescence spectrum has a certain consistency (Fig. S3†). Fig. 5B showed the influence of OTC solution with different concentrations on the fluorescence intensity of Pd NCs. It is found that the fluorescence intensity of OTC and Pd NCs solution showed a good linear quenching relationship in the concentration within 25–440 nM, the correlation coefficients were 0.9802 and 0.99 (Fig. 5C). The LOD of the proposed nanosensor for OTC was calculated to be 22 nM. The above results all proved that PEI–Pd NCs have good stability and selectivity when used in OTC detection. Compared with other reported ways for OTC detection (Table 1), the proposed strategy showed a satisfactory performance.

3.5. Fluorescence quenching mechanism

In order to clarify the reason why PEI–Pd NCs can realize the detection of OTC, the fluorescence quenching mechanism of PEI–Pd NCs was studied. The main theory of fluorescence quenching is that the emission band of the fluorescent group overlaps with the absorption band of the analyte, which leads to fluorescence quenching.[40] At the same time, the fluorescence quenching efficiency is positively correlated with the degree of overlap.[41] As shown in Fig. 6A, there is a large overlap between the absorption spectrum of OTC with the emission spectrum of Pd NCs that the observed emission quenching can occur from inner filter effect (IFE) and fluorescence resonance energy transfer (FRET) processes. Moreover, the absorption spectra of background materials (including AA PEI and Pd^{2+}) had also been studied, which would not affect the fluorescence spectra of the products (Fig. S2†). To further distinguish the IFE and FRET processes, time-resolved fluorescence lifetime experiments for PEI–Pd NCs in the presence and absence of OTC were recorded, and lifetime decay curves were collected (Fig. 6B). As shown in Fig. 6B, the fluorescence life time value for PEI–Pd NCs was 1.44 ns. After the addition of OTC to PEI–Pd NCs, very minor change

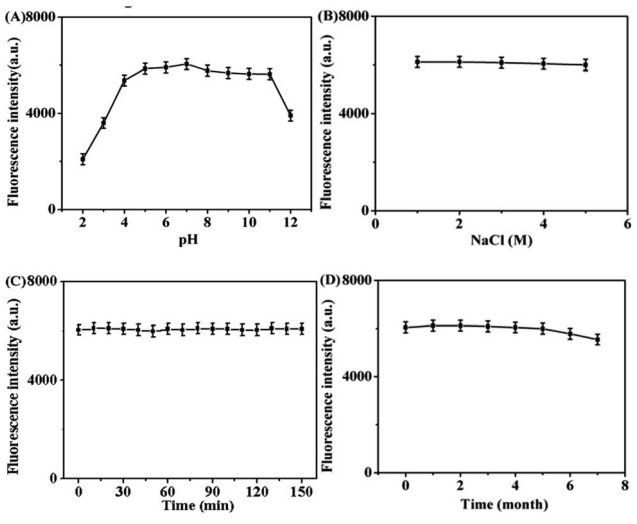

Fig. 4 Effects of different pH (A), NaCl concentration (B), light time (C), and storage time (D) on the fluorescence intensity of Pd NCs.

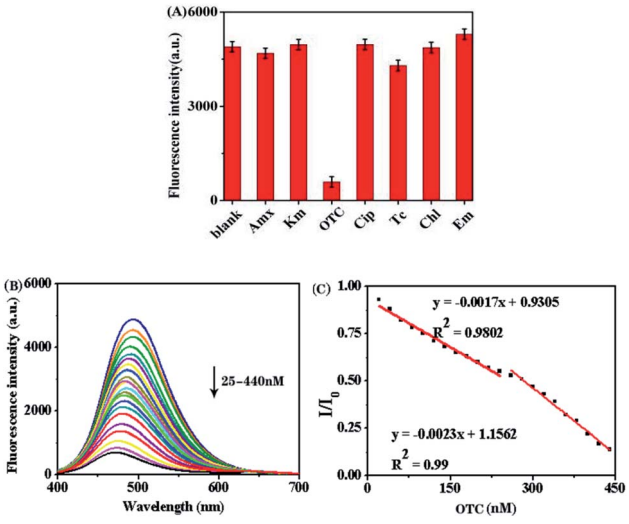

Fig. 5 (A) Selectivity experiments of Pd NCs. (B) Changes in fluorescence intensity of Pd NCs with OTC. (C) Linear plot of I/I_0 and OTC concentration.

Table 1 Comparison of this work with other reports for OTC detection

Methods	Detection range	LOD	Real samples	References
HPLC-MS	—	2 μg kg^{-1}	Pig oral fluid	12
Electrochemistry	1.0–1.0 × 10^5 μg L^{-1}	0.23 μg L^{-1}	Milk	14
Electrochemiluminescence	0.1–100 μM	0.10 μM	Drug	15
Paper test-strip	0.5–5 × 10^3 μM	30 ng mL^{-1}	Environmental water	17
Fluorescence	0.2–2 nM, 2–800 nM	0.15 nM	Milk	20
Chemiluminescence	0.075–3.0 μM	25 nM	Milk, water	38
Colorimetry	0.5–15.0 μM	0.3 μM	Rat serum	39
Fluorescence	25–440 nM	22 nM	Tap water	This work

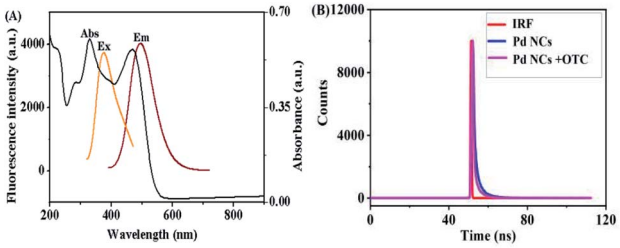

Fig. 6 (A) Excitation and emission spectra of Pd NCs and absorption spectrum of OTC. (B) Fluorescence decay curves of Pd NCs in an aqueous solution and fluorescence decay curves of OTC in the Pd NC aqueous solution.

of fluorescence decay lifetimes from 1.44 to 1.41 has occurred. FRET belongs to dynamic quenching mechanism because energy/electron transfer process can occur only in an excited state and alters the fluorescence lifetime of the fluorophore. Therefore, the dynamic quenching mechanism can be excluded in this system. Based on the experiments, it can be concluded that the quenching mechanism of the system is based on IFE.

3.6. Real sample analysis

In order to evaluate the practicability of the sensor in the actual sample, we chose tap water as the object of actual sample analysis of OTC. OTC of different concentrations was added respectively, and the samples were centrifuged at 8000 rpm min^{-1}. Finally, the recovery test was carried out. As shown in Table 2, the recovery rate reached 97.00–108.00%, the relative standard deviation (RSD, $n = 3$) was 1.70–3.80%.

4. Conclusions

In this study, fluorescent Pd NCs synthesized by PEI as a stabilizer was used as a nanosensors for the detection of OTC. The morphology, chemical structure and optical properties of Pd NCs were researched by using different characterization methods such as TEM, XPS, FTIR, UV-vis and fluorescence spectroscopy. The Pd NCs showed good optical stability under the condition of high metal ion density, continuous lighting time, various PH and long storage time, which laid the foundation for the application of Pd NCs. Based on the fluorescence resonance energy transfer technology, OTC nanobiosensor was invented, which showed extremely high selectivity, wide linear range and lower detection limitation for OTC. In addition, the present nanosensor has been successfully applied to the detection of OTC in real water samples. Considering these advantages, the proposed PEI–Pd NCs as a fluorescent nanosensor is a competitive solution for OTC detections compared to other existed methods. However, the uncontrolled toxicity or deactivation of palladium catalysts is still a huge economic burden in the chemical industry and environmental governance, as well as a focus of technical and academic research. Therefore, the development of palladium catalysts with controllable toxicity and activity is the most urgent task in this field.

Table 2 Detection of OTC in water samples

Samples	Added (nM)	Detected (nM)	Recovery (%)	RSD (%)
1	100	97.0	97.0	1.70
2	200	189.0	94.5	2.40
3	300	326.0	108.0	3.80

Conflicts of interest

There are no conflicts to declare.

Acknowledgements

The project was supported by the National Natural Science Foundation of China (21575083), Jinzhong College "1331 Project" Innovation Team (jzxycxtd2019007) the 12th "Hundred Talents Plan" in Shanxi Province (128, 129, Meng Liu), Major Science and Technology Project of Shanxi Province (No. 20191102005). And the project was also supported by a grant from Shanxi Laboratory for Yellow River. Special thanks to Doctor Li Li for her guidance on antibiotic testing in the article.

Notes and references

1 H. Douafer, V. Andrieu, O. t. Phanstiel and J. M. Brunel, *J. Med. Chem.*, 2019, **62**, 8665–8681.
2 X. Wang, J. Li, D. Jian, Y. Zhang, Y. Shan, S. Wang and F. Liu, *Sens. Actuators, B*, 2021, **329**, 129173.
3 K. Yan, Y. Liu, Y. Yang and J. Zhang, *Anal. Chem.*, 2015, **87**, 12215–12220.

4 M. Jing, H. Zhang, M. Li, Z. Mao and X. Shi, *Spectrochim. Acta, Part A*, 2021, **255**, 119652.
5 Y. Yang, G. Ren, W. Yang, X. Qin, D. Gu, Z. Liang, D.-Y. Guo and P. Qinhe, *Polyhedron*, 2021, **194**, 114923.
6 B. Ince, H. Coban, G. Turker, E. Ertekin and O. Ince, *Bioprocess Biosyst. Eng.*, 2013, **36**, 541–546.
7 *European Food Safety Authority*, 2017, vol. 14, 11, p. 1150E.
8 Y. Xiang, H. Wu, L. Li, M. Ren, H. Qie and A. Lin, *Ecotoxicol. Environ. Saf.*, 2021, **213**, 112044.
9 Z. Wang, Y. Du, C. Yang, X. Liu, J. Zhang, E. Li, Q. Zhang and X. Wang, *Sci. Total Environ.*, 2017, **609**, 1423–1432.
10 M. Bacanli and N. Basaran, *Food Chem. Toxicol.*, 2019, **125**, 462–466.
11 J. Han, D. Jiang, T. Chen, W. Jin, Z. Wu and F. Cui, *J. Chromatogr. B*, 2020, **1152**, 122253.
12 A. Gajda, A. Jablonski, T. Bladek and A. Posyniak, *J. Agric. Food Chem.*, 2017, **65**, 494–500.
13 J. Sun, T. Gan, W. Meng, Z. Shi, Z. Zhang and Y. Liu, *Anal. Lett.*, 2014, **48**, 100–115.
14 Y. Yang, W. Yan, Y. Guo, X. Wang, F. Zhang, L. Yu, C. Guo and G. Fang, *Sensors and Actuators Reports*, 2020, **2**, 100009.
15 X. Chen, L. Zhao, X. Tian, S. Lian, Z. Huang and X. Chen, *Talanta*, 2014, **129**, 26–31.
16 J. Li, S. Fan, Z. Li, Y. Xie, R. Wang, B. Ge, J. Wu and R. Wang, *Opt. Spectrosc.*, 2014, **117**, 250–255.
17 H. I. Gomes and M. G. Sales, *Biosens. Bioelectron.*, 2015, **65**, 54–61.
18 Y. Chen, D. Kong, L. Liu, S. Song, H. Kuang and C. Xu, *Food Anal. Methods*, 2015, **9**, 905–914.
19 A. L. Myllyniemi, R. Rannikko, E. Lindfors, A. Niemi and C. Backman, *Food Addit. Contam.*, 2000, **17**, 991–1000.
20 A. Bahreyni, H. Luo, M. Ramezani, M. Alibolandi, V. Soheili, N. M. Danesh, M. S. Ashjaei, K. Abnous and S. M. Taghdisi, *Spectrochim. Acta, Part A*, 2021, **246**, 119009.
21 Y. Wu, S. Zheng, Y. Ye, H. Guo and F. Yang, *J. Photochem. Photobiol., A*, 2021, **412**, 113219.
22 L. Wang, J. Zhang, D. Cui, X. Wang, Z. Yang, K. Zhang, Z. Qin, J. Meng, G. Hao and J. Li, *Anal. Lett.*, 2014, **47**, 1015–1030.
23 M. Przeniosło-Siwczyńska, E. Patyra, M. Chyłek-Purchała, B. Kozak and K. Kwiatek, *Bull. Vet. Inst. Pulawy*, 2015, **59**, 527–532.
24 Y. Yang, Y. Cao, X. Wang, G. Fang and S. Wang, *Biosens. Bioelectron.*, 2015, **64**, 247–254.
25 L. Zhang and E. Wang, *Nano Today*, 2014, **9**, 132–157.
26 J. Zheng, P. R. Nicovich and R. M. Dickson, *Annu. Rev. Phys. Chem.*, 2007, **58**, 409–431.
27 J. Mu, J.-L. Yang, D.-W. Zhang and Q. Jia, *Chinese J. Anal. Chem.*, 2021, **49**, 319–329.
28 Y. Lu and W. Chen, *Chem. Soc. Rev.*, 2012, **41**, 3594–3623.
29 T. Vosch, Y. Antoku, J. C. Hsiang, C. I. Richards, J. I. Gonzalez and R. M. Dickson, *Proc. Natl. Acad. Sci. U. S. A.*, 2007, **104**, 12616–12621.
30 S. Palmal and N. R. Jana, *Wiley Interdiscip. Rev.: Nanomed. Nanobiotechnol.*, 2014, **6**, 102–110.
31 X. Du, W. Dong, Z. Li, G. Wen, M. Liu and X. Fan, *New J. Chem.*, 2020, **44**, 9248–9254.
32 L. Naik, R. Sharma, B. Mann, K. Lata, Y. S. Rajput and B. Surendra Nath, *Food Chem.*, 2017, **219**, 85–92.
33 J. Wang, Y. Zhou, M. Zeng, Y. Zhao, X. Zuo, F. Meng, F. Lv and Y. Lu, *Environ. Res.*, 2021, **203**, 111818.
34 Z. Zhang, Y. Tian, P. Huang and F. Y. Wu, *Talanta*, 2020, **208**, 120342.
35 D. Yan, P. C. Xu, Q. Xiong, H. R. Mou, Q. Xu, W. J. Wen, X. X. Li and Y. Zhang, *J. Mater. Chem. A*, 2016, **4**(9), 3487–3493.
36 T. Zhang, H. Li, M. Liu, H. Zhou, Z. Zhang, C. Yu, C. Wang and G. Wang, *Sens. Actuators, B*, 2021, **341**, 129987.
37 C. Wang, D. Chen, Q. Wang and R. Tan, *Biosens. Bioelectron.*, 2017, **91**, 262–267.
38 M. Amjadi, T. Hallaj and F. Mirbirang, *Microchim. Acta*, 2020, **187**, 1–7.
39 X. Zhang, J. Qiao, W. Liu and L. Qi, *Analyst*, 2021, **146**, 5061–5066.
40 S. S. Nagarkar, B. Joarder, A. K. Chaudhari, S. Mukherjee and S. K. Ghosh, *Angew. Chem.*, 2013, **52**, 2881–2885.
41 B. Zhang, P. Y. Guo, L. N. Ma, B. Liu, L. Hou and Y. Y. Wang, *Inorg. Chem.*, 2020, **59**, 5231–5239.